Systematical Study of InAlN/GaN Devices by Numerical Simulation

S. Vitanov*, V. Palankovski, G. Pozzovivo[a], J. Kuzmik[a], and R. Quay[b]
Advanced Materials and Device Analysis Group,
Inst. for Microelectronics, TU Vienna, Gusshausstr. 27–29, 1040 Vienna, Austria
[a]***Inst. for Solid-State Electronics, TU Vienna, Floragasse 7, 1040 Vienna, Austria***
[b]***Fraunhofer Inst. for Solid-State Physics (IAF), Tullastr. 72, 79108 Freiburg, Germany***
*Corresponding author: vitanov@iue.tuwien.ac.at

Abstract

InAlN/GaN HEMTs have been proposed to provide higher polarization charges without the drawback of high strain [1]. Several groups have demonstrated devices based on InAlN/GaN ([2], [3]), with maximum current capabilities surpassing those of AlGaN/GaN structures. For further optimization a reliable simulation tool is needed. Our two-dimensional device simulator MINIMOS-NT *is expanded by material models for InAlN. Relying on experimental work, we conduct a simulation study of InAlN HEMTs. Using a calibrated setup, we explore device specific effects and we estimate the AC device performance.*

1. DEVICE STRUCTURE

Optimization of the structures has been carried out by using analytical models [1]. In order to fully develop the potential of the device, proper modeling of the materials is required. However, many of the material properties (e.g. bandgap bowing parameter varying from 2.5 eV up to 4.0 eV) are still subject of discussion. Based on our previous work on InN and AlN we introduce a material model for InAlN, which is then incorporated in the two-dimensional device simulator MINIMOS-NT, thus enabling the simulation and optimization of novel InAlN/GaN structures. We use HEMT structures described in [3] and [4] to benchmark the DC and AC simulation results against measured data. Schematic layer structure of the investigated $In_{0.2}Al_{0.8}N$/GaN device [4] is shown in Fig. 1. All layers are non-intentionally doped.

2. DEVICE MODELING AND SIMULATION RESULTS

Since the longitudinal electric fields in the channel reach high peak values [5], we employ a hydrodynamic transport model. We assume a bandgap bowing factor of 3 eV for InAlN. This yields a bandgap of 4.58 eV for $In_{0.2}Al_{0.8}N$ at 300 K (Fig. 2). The values for the band offsets are ΔE_C=0.66 eV and ΔE_V=0.59 eV, corresponding to a 53%/47% setup. The calculated dielectric permittivity of $In_{0.2}Al_{0.8}N$ is 9.86, which is in a good agreement with the value listed in [4]. The barrier height of the gate Schottky contact is 1 eV. The value of the sheet charge at the InAlN/GaN interface induced by the polarization effects is found to be 3.3×10^{13} cm^{-2} from the DC characteristics (simulation results for different values are given in Fig. 3). A commensurate negative surface charge (as the device is not passivated, a low value of 1.0×10^{13} cm^{-2} is assumed) at the top of the InAlN surface is also considered in the simulation. Simulation results for the transfer characteristics assessing different charge values are shown in Fig. 4. Self-heating effects are accounted for by using thermal resistance of R_{th}=3 K/W at the substrate thermal contact (Fig. 5 compares transfer characteristics without self-heating effects and with different values of R_{th}). This value lumps the thermal resistance of the nucleation layer and the sapphire substrate, and possible three-dimensional thermal effects. Our simulation exhibits good agreement with the experimental data under consideration of ohmic contact resistances R_C=1.3 Ωmm. Simulated output characteristics show a good agreement with the experimental data (Fig. 6). By AC analysis of the device, cut-off frequency $f_T\approx$7 GHz is obtained. This low value can be explained with the conservative design of the device and the low carrier mobility in the channel (μ=230 cm^2/Vs). Downscaled devices are analyzed (l_g=0.5/0.25 μm) and the effect of higher quality GaN material on AC performance is studied. In another simulation, a l_g=0.25 μm device reported in [3] (carrier mobility μ=530 cm^2/Vs) reaches f_T=36 GHz.

The authors acknowledge support from the Austrian Science Fund (FWF), Project START Y247-N13.

[1] J. Kuzmik, "Power Electronics on InAlN/(In)GaN: Prospect for a Record Performance", in *IEEE Electron Device Lett.*, vol. 22, no. 11, pp. 510–513, 2001.

[2] M. Hiroki, H. Yokoyama, N. Watanabe, and T. Kobayashi, "High-Quality InalN/GaN Heterostructures Grown by Metal-Organic Vapor Phase Epitaxy", in *Superlattices & Microstructures*, vol. 40, no. 4–6, pp. 214–218, 2006.

[3] F. Medjdoub, N. Sarazin, M. Tordjman, M. Magis, M. di Forte-Poisson, M. Knez, E. Delos, C. Gaquiere, S. Delage, and E. Kohn, "Characteristics of Al_2O_3/AlInN/GaN MOSHEMT", in *Electron.Lett.*, vol. 43, no. 12, pp. 691–692, 2007.

[4] J. Kuzmik, A. Kostopoulos, G. Konstantinidis, J. Carlin, A. Georgakilas, and D. Pogany, "InAlN/GaN HEMTs: A First Insight Into Technological Optimization", in *IEEE Trans.Electron Devices*, vol. 53, no. 3, pp. 422–426, 2006.

[5] V. Palankovski, S. Vitanov, and R. Quay, "Field-Plate Optimization of AlGaN/GaN HEMTs", in *Tech.Dig. IEEE Compound Semiconductor IC Symp.*, pp. 107–110, 2006.

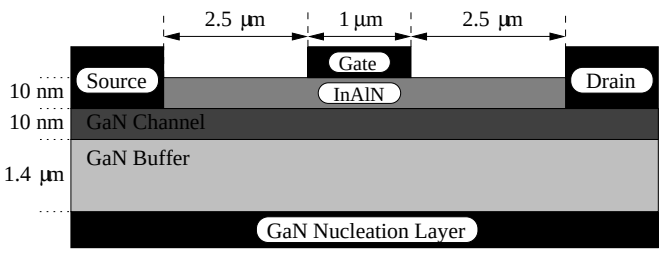

Fig. 1: Schematic layer structure of the investigated device.

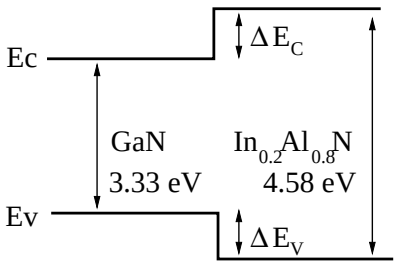

Fig. 2: Band alignment of the heterointerface.

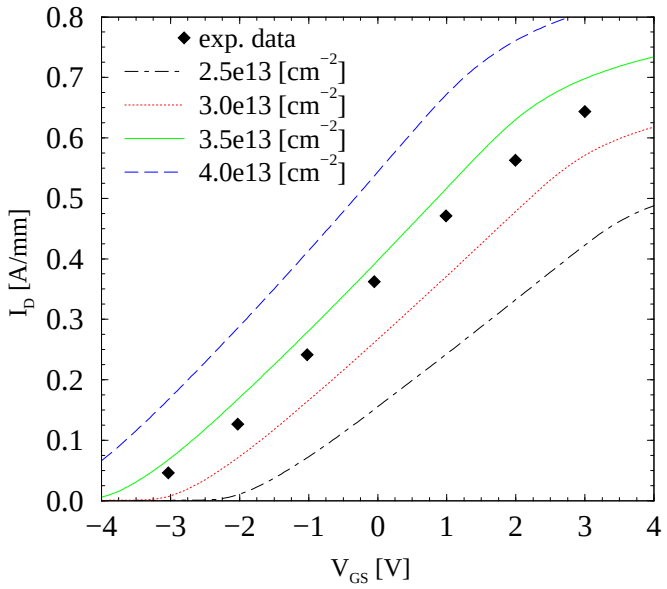

Fig. 3: Transfer characteristics for different values of the polarization charge at the InAlN/GaN interface and -1.0×10^{13} cm^{-2} at the top of the InAlN interface (V_{ds}=8.0 V).

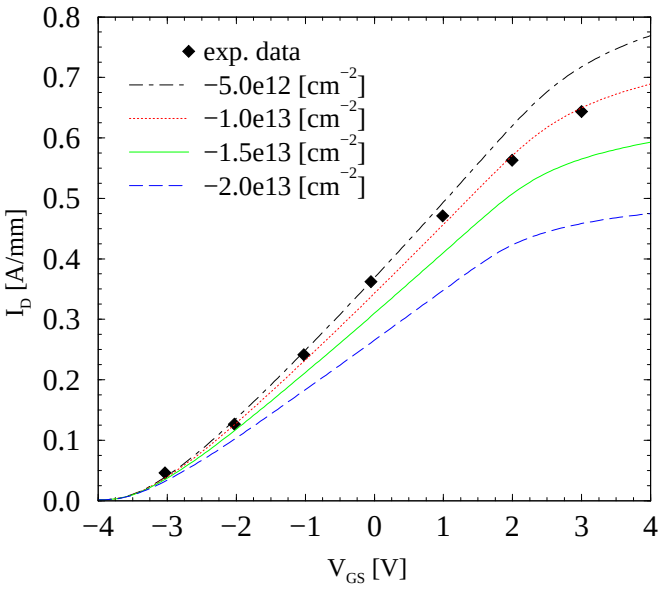

Fig. 4: Transfer characteristics for different values of the total charges (polarization and traps) at the top of the InAlN surface and 3.3×10^{13} cm^{-2} at the InAlN/GaN interface (V_{ds}=8.0 V).

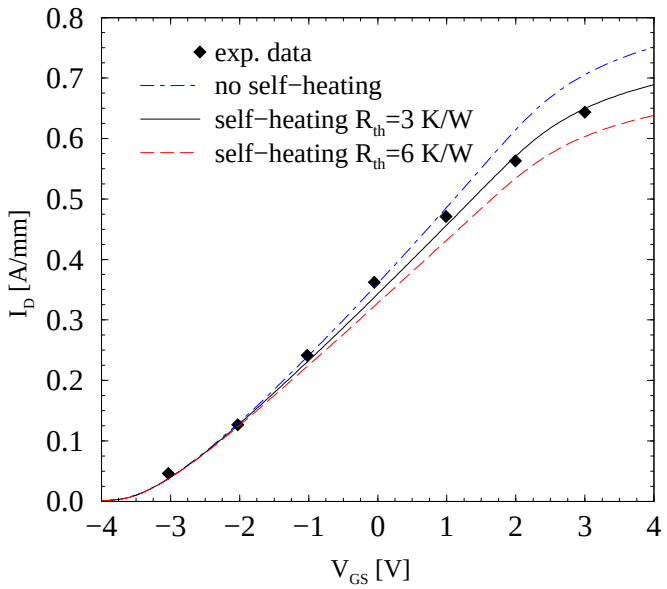

Fig. 5: Comparison of simulated transfer characteristics for different values of the thermal resistance and experimental data (V_{ds}=8.0 V).

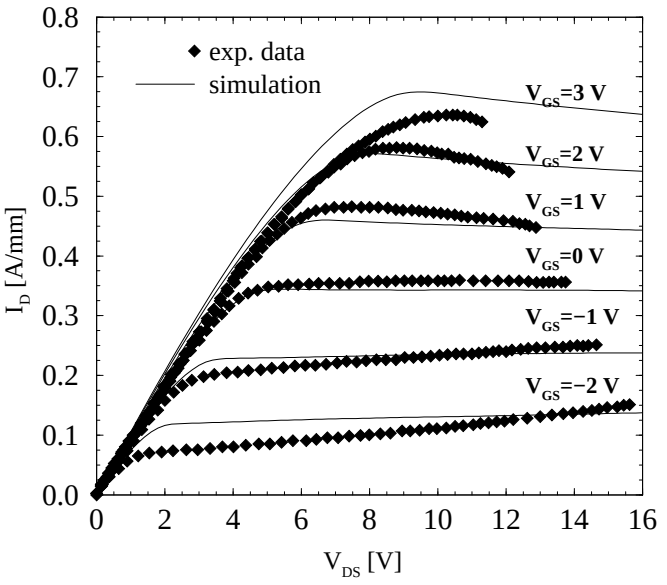

Fig. 6: Comparison of simulated output characteristics and experimental data.